

## Dynamic Chirp Control and Pulse Compression for Attosecond High-Order Harmonic Emission

Yinghui Zheng, Zhinan Zeng,\* Pu Zou, Li Zhang, Xiaofang Li, Peng Liu, Ruxin Li,† and Zhizhan Xu‡

State Key Laboratory of High Field Laser Physics, Shanghai Institute of Optics and Fine Mechanics, Chinese Academy of Sciences, Shanghai, 201800, China

(Received 8 February 2009; published 23 July 2009)

We propose a scheme to compensate dynamically the intrinsic chirp of the attosecond harmonic pulses. By adding a weak second harmonic laser field to the driving laser field, the chirp compensation can be varied from the negative to the positive continuously by simply adjusting the relative time delay between the two-color pulses. Using this technique, the compensation of the negative chirp in harmonic emission is demonstrated experimentally for the first time and the nearly transform-limited attosecond pulse trains are obtained.

DOI: 10.1103/PhysRevLett.103.043904

PACS numbers: 42.65.Ky, 32.80.Rm

High-order harmonic generation (HHG) and the attosecond pulse emission based on HHG have been extensively investigated in recent years [1,2]. The successful isolation of only one trajectory for the returning electrons during HHG can offer a wide-band extreme-ultraviolet (XUV) supercontinuum. However, the attainable shortest attosecond pulse duration is further limited by the intrinsic chirp of the harmonic emission, which is originated from the laser-intensity-dependent atomic dipole phase [2,3]. Consequently, the phase control and chirp compensation of attosecond harmonic pulses are of vital importance for producing the transform-limited (TL) attosecond pulses.

Three techniques have so far been proposed to manipulate the chirp of harmonic pulses, including the use of chirped multilayer x-ray mirrors [4], and to employ the negative group delay dispersion (GDD) either in a thin metallic foil [2,5] or in a thick gas medium [6] through which the harmonic emission is transported. The former is difficult to implement experimentally. The latter relies on the dispersion characteristic of the transmission material, a tradeoff between the absorption and the available negative GDD should be made, which limits the spectral region suitable for chirp compensation. Moreover, all the above techniques are based on the static dispersion characteristics of materials and only the positive chirp has so far been compensated experimentally. Since suitable materials with positive GDD are needed, the compensation of negative chirp is very difficult to achieve in the XUV region.

In this Letter we demonstrate a new scheme by exploiting the dispersion characteristic controlled by the employed laser field, to compensate the intrinsic chirp of the attosecond harmonic pulses, which is referred as the dynamic compensation of chirp here in this work, different from previous approaches based on the static dispersion of the materials. To control the intrinsic chirp of the harmonic generation, we add a weak second harmonic (SH) laser pulse to the fundamental driving laser pulse for HHG, the chirp compensation can be varied from the negative to the positive continuously by simply adjusting the relative time delay between the two-color pulses.

As we know, the intrinsic harmonic chirp is positive and negative for the harmonic emission due to the short and long trajectories, respectively [7]. When the gas medium for HHG is placed behind the laser focus, the short trajectory is favored and the generated harmonic pulses are positively chirped. Nevertheless, in order to generate strong harmonic pulses, using a self-guided driving laser beam is an effective method [8,9] in which the gas medium is placed before or at the laser focus so that both the short and long trajectories are contributing significantly. In this case, the intrinsic chirp of the harmonic emission is rather complicated. The compensation technique for both the positive and negative chirps is highly desired.

The two-color scheme for HHG has recently been investigated extensively [10–19]. The additional phase induced by the SH field was analyzed and an approach to control the birth of the attosecond pulse has been demonstrated [15]. As shown in Ref. [15], if the SH field is much weaker than the fundamental field, the action in the two-color field can be written as

$$\begin{aligned} S_2(t, \phi) &= S_1(t) - \sigma(t, \phi) \\ &= S_1(t) - \int_{t'(t)}^t \vec{v}_{\text{SFA}}(\tau, t') \vec{A}_2(\tau, \phi) d\tau, \end{aligned} \quad (1)$$

where  $S_1$  is the unperturbed action,  $\sigma$  is the additional phase induced by the second field,  $\vec{v}_{\text{SFA}}$  is the velocity of the unperturbed trajectory, which starts with zero velocity at the moment of ionization  $t'(t)$  and returns at  $t$ , and includes only the effect of the fundamental laser field.  $\vec{A}_2(\tau, \phi) = A_2 \sin(2\omega\tau + \phi)$  is the vector potential of the SH field and  $\phi$  is the relative phase between the two-color laser field which can be altered by changing the time delay between the two pulses. Therefore  $\vec{A}_2(\tau, \phi + \pi) = -\vec{A}_2(\tau, \phi)$ , which means if the  $\vec{A}_2(\tau, \phi)$  can contribute the positive GDD, then the  $\vec{A}_2(\tau, \phi + \pi)$  can contribute the negative GDD by simply changing the time delay between the fundamental and SH laser pulses.

It is obvious that when the relative phase between the fundamental and the SH fields is changed, the phases of the generated high-order harmonics follow to change. As shown in Fig. 1(a), the calculated phase of the 25th harmonic in argon varies periodically with a period of 1.33 fs when the time delay between the 50 fs fundamental (800 nm) and the SH (400 nm) pulses is varied continuously from 0 to 2.67 fs (one cycle of 800 nm laser). The calculations are done based on the Lewenstein model [20] and the saddle-point method. In the calculations, the intensities of the fundamental and the SH pulses are  $2 \times 10^{14}$  and  $3 \times 10^{12}$  W/cm<sup>2</sup>, respectively. We then calculate the attosecond chirp for the 19th to 29th harmonics in argon as a function of the time delay between the two-color pulses and the results are shown in Fig. 1(b). Under the given laser condition, the optimum time delay is 0.42 fs and the corresponding attosecond chirp is  $5.7 \times 10^{-3}$  fs<sup>2</sup>, which can support a nearly TL attosecond pulse train.

The schematic experimental setup is shown in Fig. 2. The 50 fs, 800 nm laser pulses at a repetition rate of 1 kHz, delivered by a commercial Ti:sapphire laser system [Legend-USP-HE, Coherent Inc.] are focused by a lens (with a focal length of 800 mm) into a 1.5 mm long argon gas cell with the pressure of 40 Torr for generating high-order harmonics. The laser focus is located 1.5 mm after the entrance of the gas cell. The optical setup for generating two-color pulses is placed between the lens and the gas cell. The SH pulses are produced using a 300  $\mu$ m type I  $\beta$ -barium borate (BBO) crystal. The remaining fundamental and the orthogonally-polarized SH pulses subsequently

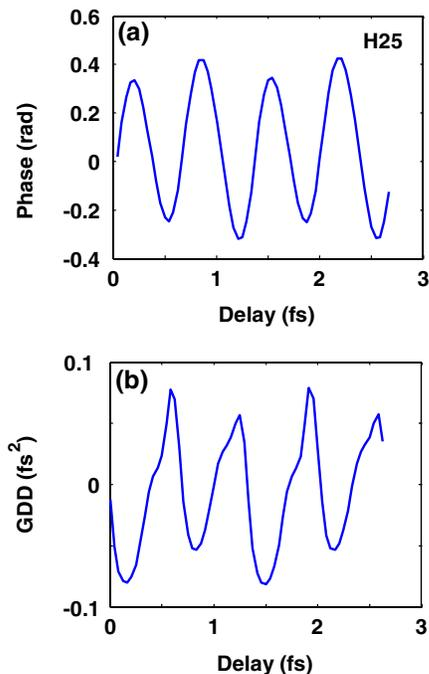


FIG. 1 (color online). (a) Calculated phase of the 25th harmonic in argon (b) Calculated attosecond chirp for the 19th to 29th harmonics as functions of the time delay between the fundamental and the SH pulses.

pass through a 0.5 mm thick quartz plate. The relative time delay between the fundamental and the SH pulses can be varied by rotating this plate. Then the delay-controlled two-color pulses pass through a 43  $\mu$ m thick zero-order wave plate that acts as a half-wave plate for the fundamental and a full-wave plate for the SH pulses, and thus we can continuously rotate the polarization direction of the fundamental pulses while maintaining the polarization of the SH pulses. The effective intensities of the fundamental and the SH pulses at the focus are estimated to be  $2 \times 10^{14}$  and  $3 \times 10^{12}$  W/cm<sup>2</sup>, respectively.

After harmonic generation, a 500 nm thick aluminum strip is placed on-axis so that only the central part of the laser beam is blocked while the remaining part can go through freely to be a probe pulse for the temporal characterization of the harmonic emission in the next stage. The outer annular harmonic beam is subsequently eliminated by a 0.1 mm thick quartz plate with a hole (3 mm in diameter) in the center. This simple setup allows only the central harmonic and the outer annular laser beams to transmit freely. Both of the laser and harmonic beams are then focused by using gold-coated mirrors into a helium gas jet for the cross correlation measurement. The generated photoelectrons from the ionized helium atoms are analyzed with a magnetic-bottle time-of-flight (TOF) electron spectrometer. In addition, a special-made gold-coated mirror as shown in Fig. 2 is used to adjust the relative phase between the harmonic and the probe laser pulses.

The spectral phase of harmonics is measured by using the method of reconstruction of attosecond beating by interference of two photon transitions (RABITT) [21]. The spectral phase difference between adjacent harmonics is inferred by measuring the phase dependence of sideband peaks occurring between the harmonic photoionization signals in the photoelectron spectrum. The amplitude information of the harmonics can be obtained from the harmonics spectra measured by a flat-field grating spectrometer with a soft-x-ray CCD detector. The temporal structure of the attosecond pulse train can then be reconstructed from the measured harmonic phase and amplitude. Furthermore, the chirp feature of the harmonic pulses can also be obtained from the spectral phase information. The high-order harmonic spectrum measured by the grating spectrometer from the argon cell with a gas pressure of 40 torr is presented in Fig. 3. It can be seen that the strong odd harmonics are accompanied by the weak even harmonics

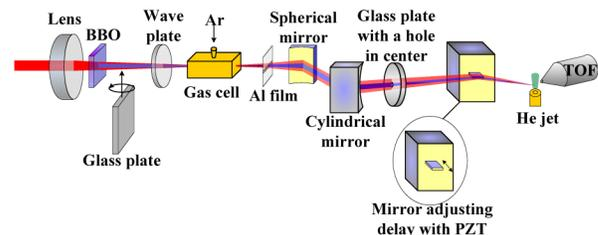


FIG. 2 (color online). Schematic of the experimental setup.

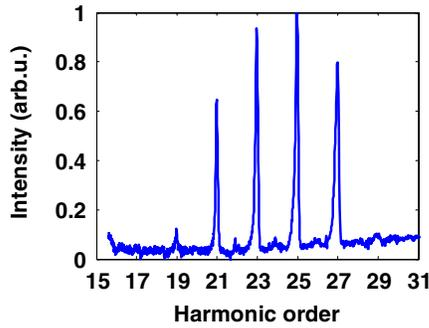


FIG. 3 (color online). Measured harmonic spectrum from the argon cell.

ics occurring between the odd ones, which is due to the two-color driving field. One can extract the relative amplitude information of the 19th to the 29th harmonics from the spectrum.

Figures 4(a) and 4(b) show the measured spectral phase difference between adjacent harmonics from the 19th to the 29th harmonics when the two-color pulses are parallel and orthogonal polarized with each other, respectively, where the labels A–D denote the gradually increased time delay between the two-color pulses starting from A. Because of the 0.5 mm thick quartz plate, the zero delay between the two color pulses cannot be obtained and, consequently, the absolute time delay cannot be determined. The relative time delays with regard to delay A for delays B, C, D are 0.0535, 0.2176, 0.4691 fs, respectively. “S” denotes that only the fundamental laser pulse is used to drive the gas cell for HHG.

Here, the spectral phase difference is a relative value, thus the effective part is the slope of the spectral phase difference, the so-called the second-order spectral phase, corresponding to the intrinsic harmonic chirp. In the figure,

the negative slope indicates that the harmonic pulses are negative chirp. The second-order spectral phase, measured by the slope of the linear fit from the 19th to the 29th order is  $5.0 \times 10^{-3} \text{ fs}^2$  at the delay B, while the second-order spectral phases at the delay A, C, D are  $1.5 \times 10^{-2} \text{ fs}^2$ ,  $2.4 \times 10^{-2} \text{ fs}^2$ , and  $2.6 \times 10^{-2} \text{ fs}^2$ , respectively. The second-order spectral phase for the case of single color driving laser pulse is  $1.3 \times 10^{-2} \text{ fs}^2$ . It can be seen that the chirp distribution is complicated in the case of single 800 nm driving laser pulse and the chirp can be compensated obviously after introducing the weak SH laser pulse at an optimized delay labeled by delay B. This implies that adjusting the relative time delay between the fundamental and the SH field can compensate the intrinsic chirp of the harmonic pulses. The results obtained by using the two-color pulses with parallel and orthogonal polarization are similar, but the higher order spectral phases are a little bit higher in the case of orthogonal polarization.

The reconstructed waveforms of the attosecond pulse trains are shown in Figs. 4(c) and 4(d), corresponding to the two-color laser pulses with parallel and orthogonal polarizations, respectively. In Fig. 4(c), the shortest pulse duration (FWHM) is about 231 as, corresponding to the delay B in Fig. 4(a). Similarly, the shortest pulse duration is 229 as in Fig. 4(d). It is very close to the TL value of 220 as. We have therefore compensated the negative chirp for the first time to the best of our knowledge, and obtained nearly TL attosecond pulses.

The harmonic bandwidth in this experiment is limited due to the phase matching and absorption process in the gas cell. Nevertheless, the chirp control scheme can deal with a much wider bandwidth corresponding to an isolated attosecond pulse shorter than 100 as. As an example, we show the calculated results of chirp compensation for the ultrabroad harmonic supercontinuum ranging from

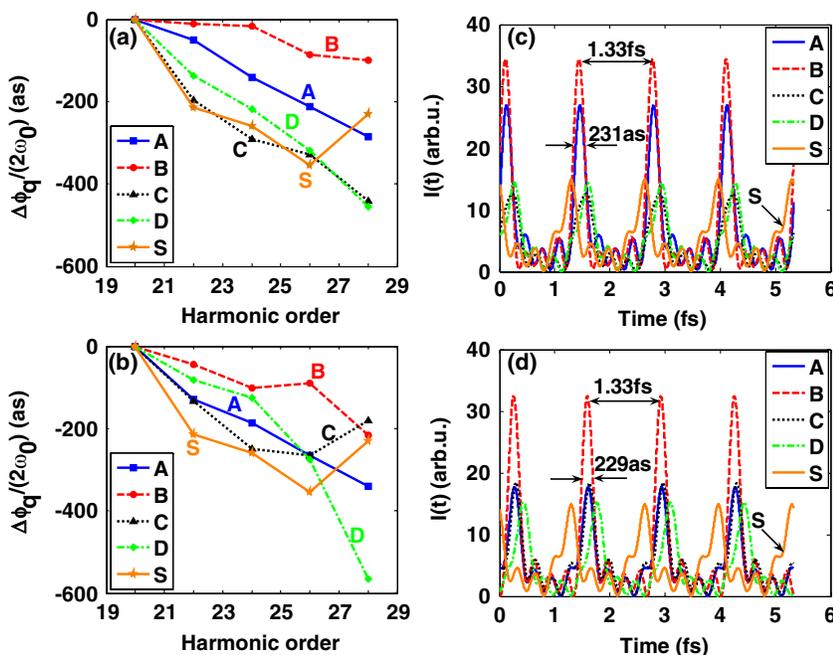


FIG. 4 (color online). (a) and (b) Measured spectral phase difference between the adjacent harmonics from the 19th to the 29th harmonics. (c) and (d) Reconstructed waveforms of the attosecond harmonic pulse trains. In (a) and (c) the two-color laser pulses are polarized parallelly, while in (b) and (d) they are polarized orthogonally.

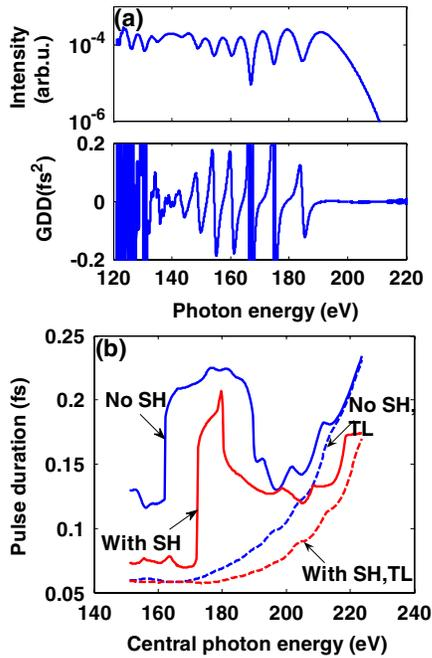


FIG. 5 (color online). (a) The XUV supercontinuum (upper panel) and the corresponding chirp (lower panel). (b) The calculated attosecond pulse duration (solid lines) and the corresponding TL pulse duration (dashed lines) as functions of central photon energy, obtained with (red lines) and without (blue lines) using a properly delayed weak 400 nm laser pulse.

120 to 220 eV obtained in our previous work [22]. The XUV supercontinuum including both the contributions from the short and long trajectories and the corresponding GDD are shown in Fig. 5(a). One can see the interference-induced intensity modulation in the spectrum and some sudden changes in GDD at the positions of destructive interference. We use a properly delayed weak ( $5 \times 10^{12}$  W/cm<sup>2</sup>) 400 nm laser pulse to compensate such a complicated chirp and the attosecond pulse durations before and after the chirp compensation are shown in Fig. 5(b).

The bandwidth is chosen as 60 eV for calculating the pulse duration. For example, the pulse duration for the central photon energy 160 eV is calculated by performing Fourier transformation for the supercontinuum ranging from 130 to 190 eV. The full width at half maximum intensity of the temporal profile of the harmonic emission is defined as the pulse duration. As can be seen in Fig. 5(b), the pulse duration is about 75 as after chirp compensation, very close to the TL pulse duration as 60 as, when the central photon energy of the attosecond pulse is in the region from 150 to 170 eV. Without the chirp compensation made by the 400 nm laser pulse, the pulse duration is

about 120 as for the central photon energies ranging from 150 to 162 eV and the pulse duration becomes 210 as for the higher photon energy region.

Adding an appropriate weak SH pulse at proper time delay to the strong fundamental driving laser pulse for HHG usually leads to considerable enhancement of harmonic yield [11,16,17] due to the increase in the peak instantaneous laser field, in accordance with this experiment. This is a unique advantage of the chirp control using two-color field, in addition to avoiding the absorption loss in the chirp compensation materials [2,5].

In conclusion, we have demonstrated a new scheme for the chirp compensation and pulse compression in HHG by adding a weak second harmonic laser field to the fundamental laser field for HHG. A nearly transform-limited attosecond pulse train has been produced by using the two-color laser pulses with an appropriate relative time delay. This technique can also be used for the generation of strong transform-limited isolated attosecond pulses.

This work is supported by the NSF of China (No. 10734080, No. 60578049, No. 10523003), the 973 Program (No. 2006CB806000), the Chinese Academy of Sciences.

\*zhinan\_zeng@siom.ac.cn

†ruxinli@mail.shenc.ac.cn

‡zzxu@mail.shenc.ac.cn

- [1] M. Hentschel *et al.*, Nature (London) **414**, 509 (2001); C. Gohle *et al.*, Nature (London) **436**, 234 (2005).
- [2] Y. Mairesse *et al.*, Science **302**, 1540 (2003).
- [3] T. Sekikawa *et al.*, Phys. Rev. Lett. **83**, 2564 (1999).
- [4] A. Morlens *et al.*, Opt. Lett. **30**, 1554 (2005).
- [5] R. López-Martens *et al.*, Phys. Rev. Lett. **94**, 033001 (2005).
- [6] K. T. Kim *et al.*, Phys. Rev. Lett. **99**, 223904 (2007).
- [7] S. Kazamias and Ph. Balcou, Phys. Rev. A **69**, 063416 (2004).
- [8] V. Tosa *et al.*, Phys. Rev. A **67**, 063817 (2003).
- [9] H. T. Kim *et al.*, Phys. Rev. A **69**, 031805(R) (2004).
- [10] I. J. Kim *et al.*, Phys. Rev. Lett. **94**, 243901 (2005).
- [11] T. T. Liu *et al.*, Phys. Rev. A **73**, 063823 (2006).
- [12] I. J. Kim *et al.*, Appl. Phys. Lett. **92**, 021125 (2008).
- [13] Y. Oishi *et al.*, Opt. Express **14**, 7230 (2006).
- [14] Z. Zeng *et al.*, Phys. Rev. Lett. **98**, 203901 (2007).
- [15] N. Dudovich *et al.*, Nature Phys. **2**, 781 (2006).
- [16] H. Mashiko *et al.*, Phys. Rev. Lett. **100**, 103906 (2008).
- [17] Y. Zheng *et al.*, Opt. Lett. **33**, 234 (2008).
- [18] E. Mansten *et al.*, New J. Phys. **10**, 083041 (2008).
- [19] N. Ishii *et al.*, Opt. Express **16**, 20876 (2008).
- [20] M. Lewenstein *et al.*, Phys. Rev. A **49**, 2117 (1994).
- [21] P. M. Paul *et al.*, Science **292**, 1689 (2001).
- [22] X. Song *et al.*, Phys. Rev. A **76**, 043830 (2007).